

Dynamics of Non-Markovianity, Quantum Correlations and Information Scrambling of Three Qubits Systems Interacting via Rashba Interaction

Nasser Metwally^{1,2*}, Fawzeya Ebrahim¹

¹Department of Mathematics, College of Science, University of Bahrain, Zallaq, Bahrain

²Department of Mathematics, Aswan University, Aswan, Egypt

Email: *nmetwally@gmail.com

How to cite this paper: Metwally, N. and Ebrahim, F. (2024) Dynamics of Non-Markovianity, Quantum Correlations and Information Scrambling of Three Qubits Systems Interacting via Rashba Interaction. *Journal of Quantum Information Science*, 14, 52-67.

<https://doi.org/10.4236/jqis.2024.142004>

Received: February 4, 2024

Accepted: April 15, 2024

Published: April 18, 2024

Copyright © 2024 by author(s) and Scientific Research Publishing Inc.

This work is licensed under the Creative Commons Attribution International License (CC BY 4.0).

<http://creativecommons.org/licenses/by/4.0/>



Open Access

Abstract

The behavior of the quantum correlations, information scrambling and the non-Markovianity of three entangling qubits systems via Rashba is discussed. The results showed that, the three physical quantities oscillate between their upper and lower bounds, where the number of oscillations increases as the Rashba interaction strength increases. The exchanging rate of these three quantities depends on the Rashba strength, and whether the entangled state is generated via direct/indirect interaction. Moreover, the coherence parameter can be used as a control parameter to maximize or minimize the three physical quantities.

Keywords

Markovianity, Correlations, Rashba Interaction, Scrambling Information

1. Introduction

Entanglement plays an essential role in some branches of quantum technology like quantum information [1], quantum communication [2], and quantum coding [3] [4]. Entanglement is very sensitive to the environments in which its applications may be achieved. Keeping the long lived entanglement between interacting qubits is one of the challenges that face the development of some important applications. In reality, it is difficult to isolate quantum systems from their ambient environments, and consequently, the decoherence of some properties of these quantum systems is expected [5] [6] [7]. There are some efforts have been introduced to discuss the entanglement's behavior for different open quantum

systems. It is shown that this property may decay, death [8] [9] sudden change [10], frozen [11], and thawed [12].

Due to the decoherence, quantum systems may lose their memory and information, but some of them can restore their lost information [13]. It has been shown that, the non-Markovian process affects the system's coherence [14]. Therefore, the non-Markovianity has become very important and has been studied for both continuous and discrete quantum systems [15]. Based on the non-Markovianity of the system, there will be an exchange of the quantum correlations and the information between the interacting systems [16].

There are some known interactions that have been used to generate entanglement between different qubit systems. Among of these interaction is Dzyaloshinskii-Moriya (DM) [17] [18] [19], Dipolar interaction [20] [21]. Moreover, Rashba interaction [7] [22] is used in many applications of quantum information. In this manuscript, we are motivated to examine the effect of Rashba interaction on the exchanging process of the quantum correlations and the information between a three qubits system.

The outline of this paper is organized as follows: In Sec. 2, we introduce the model of the qubits-system and its time evolution analytically. The dynamic of the quantum correlations is discussed in Sec. 3, where we used the negativity as a quantifier of the quantum correlations. Sec. 4 is devoted to investigating the non-Markovianity of each two-qubit system. The behavior of the encoded information in each partition is considered in Sec. 5. Finally, the obtained results are summarized in Sec. 6.

2. Suggested Model

The suggested system consists of two qubits A , and B , which have been prepared in a partial entangled state, ρ_{AB} . The dynamic of system is governed by a Heisenberg XX spin model. It is assumed that, one terminal of the system ρ_{AB} , say the subsystem A , interacts locally with a third qubit C , via Rashba interaction [7] [22]. The total Hamiltonian which describes this system is given by,

$$\hat{\mathcal{H}}_{\text{sys}} = \hat{\mathcal{H}}_{\text{Heis}} + \hat{\mathcal{H}}_{\text{Rash}}, \quad (1)$$

where $\mathcal{H}_{\text{Heis}}$ represents the Hamiltonian of the spin XX Heisenberg interaction between the two qubits A , B , and $\mathcal{H}_{\text{Rash}}$ represents the Hamiltonian of the Rashba interaction between qubits A and C . Mathematically, these Hamiltonians are described by,

$$\begin{aligned} \mathcal{H}_{\text{Heis}} &= \frac{1}{2} \omega (\sigma_A^x \sigma_B^x + \sigma_A^y \sigma_B^y), \\ \mathcal{H}_{\text{Rash}} &= \frac{\varepsilon}{2} (I \otimes \sigma_z^C) + \beta (\tau_x^A \otimes I) - \zeta (\tau_y^A \otimes \sigma_x^C), \end{aligned} \quad (2)$$

where σ_i, τ_j , $i, j = x, y, z$ represent Pauli operators, ω is the coupling parameter between the qubits A and B , ε is the Zeeman splitting generated by an external constant magnetic field along the z -axis, β is the strength of the

tunneling coupling between the two qubits A and C , and ζ is the interaction strength, and the spin-flip tunnel coupling [18]. Let us assume that the initial state of the whole system at time $t = 0$ is given by,

$$\rho_s(0) = \rho^{AB}(0) \otimes \rho^C(0), \tag{3}$$

where,

$$\rho^{AB}(0) = \kappa |\varphi^{ab}\rangle\langle\varphi^{ab}| - \frac{1}{4}(1-\kappa)I_{4 \times 4}, \quad \rho^C(0) = |\varphi^c\rangle\langle\varphi^c|, \tag{4}$$

with $|\varphi^{AB}\rangle = \cos(\alpha)|eg\rangle + \sin(\alpha)|ge\rangle$, and $|\varphi^c\rangle = \cos(\gamma)|e\rangle + \sin(\gamma)|g\rangle$, $I_{4 \times 4}$ is the identity matrix. The time evaluation of the system at any arbitrary time t is given by,

$$\rho_s(t) = \mathcal{U}(t)\rho_s(0)\mathcal{U}(t)^\dagger, \mathcal{U}(t) = \exp[-i\mathcal{H}_{\text{sys}}t]. \tag{5}$$

Then by using the unitary operator $\mathcal{U}(t)$ and the initial state $\rho_s(0)$, one gets the final state $\rho_s(t)$ at any $t > 0$. Now, we can obtain the state between each two subsystems by tracing the third system, namely $\rho_{ij} = \text{Tr}_k\{\rho_{ijk}\}$. For example $\rho_{AC} = \text{Tr}_B\{\rho_{ABC}\}$. However, the mathematical expressions of these states are too long to be written in the manuscript. The unitary operator of the system may be written explicitly as,

$$\mathcal{U}(t) = \begin{pmatrix} u_{00} & u_{01} & u_{02} & u_{03} & u_{04} & u_{05} & u_{06} & u_{07} \\ u_{10} & u_{11} & u_{12} & u_{13} & u_{14} & u_{15} & u_{16} & u_{17} \\ u_{20} & u_{21} & u_{22} & u_{23} & u_{24} & u_{25} & u_{26} & u_{27} \\ u_{30} & u_{31} & u_{32} & u_{33} & u_{34} & u_{35} & u_{36} & u_{37} \\ u_{40} & u_{41} & u_{42} & u_{43} & u_{44} & u_{45} & u_{46} & u_{47} \\ u_{50} & u_{51} & u_{52} & u_{53} & u_{54} & u_{55} & u_{56} & u_{57} \\ u_{60} & u_{61} & u_{62} & u_{63} & u_{64} & u_{65} & u_{66} & u_{67} \\ u_{70} & u_{71} & u_{72} & u_{73} & u_{74} & u_{75} & u_{76} & u_{77} \end{pmatrix}, \tag{6}$$

where the elements u_{ij} are given by,

$$\begin{aligned} u_{00} &= \mu_- C_\beta C_\zeta, & u_{01} &= i\mu_- S_\beta S_\zeta, & u_{04} &= -i\mu_- C_\zeta S_\beta, & u_{05} &= \mu_- C_\beta S_\zeta, \\ u_{10} &= i\mu_+ S_\beta S_\zeta, & u_{11} &= i\mu_+ C_\beta C_\zeta, & u_{14} &= i\mu_+ C_\beta S_\zeta, & u_{15} &= -i\mu_+ C_\zeta S_\beta, \\ u_{20} &= -\mu_- C_\zeta S_\omega S_\beta, & u_{21} &= i\mu_- C_\beta S_\omega S_\zeta, & u_{22} &= i\mu_- C_\beta C_\omega C_\zeta, & u_{23} &= i\mu_- C_\omega S_\beta S_\zeta, \\ u_{24} &= -i\mu_- C_\beta C_\zeta S_\omega, & u_{25} &= -\mu_- S_\omega S_\beta S_\zeta, & u_{26} &= -i\mu_- C_\omega C_\zeta S_\beta, & u_{27} &= \mu_- C_\omega C_\beta S_\zeta, \\ u_{30} &= i\mu_+ C_\beta S_\omega S_\zeta, & u_{31} &= -\mu_+ C_\zeta S_\omega S_\beta, & u_{32} &= i\mu_+ C_\omega S_\beta S_\zeta, & u_{33} &= \mu_+ C_\beta C_\omega C_\zeta, \\ u_{34} &= -\mu_+ S_\omega S_\beta S_\zeta, & u_{35} &= -i\mu_+ C_\beta C_\zeta S_\omega, & u_{36} &= \mu_+ C_\omega C_\beta S_\zeta, & u_{37} &= -i\mu_+ C_\omega C_\zeta S_\beta, \end{aligned} \tag{7}$$

where, $C_\beta = \cos(\beta t)$, $S_\beta = \sin(\beta t)$, $C_\omega = \cos(\omega t)$, $S_\omega = \sin(\omega t)$,

$C_\zeta = \cos(\zeta t)$, $S_\zeta = \sin(\zeta t)$, and $\mu_\pm = \cos\left(\frac{t\mathcal{E}}{2}\right) \pm i\sin\left(\frac{t\mathcal{E}}{2}\right)$. The remaining elements of the unitary operator are given by \mathcal{U}_t ,

$$\begin{aligned} u_{40} &= u_{26}, & u_{41} &= -u_{27}, & u_{42} &= u_{24}, & u_{43} &= -u_{25}, & u_{44} &= u_{22}, & u_{45} &= -u_{23}, \\ u_{46} &= u_{20}, & u_{47} &= -u_{21}, & u_{50} &= -u_{36}, & u_{51} &= u_{37}, & u_{52} &= -u_{34}, & u_{53} &= -u_{25}, \\ u_{54} &= -u_{32}, & u_{55} &= u_{33}, & u_{56} &= -u_{30}, & u_{57} &= u_{31}, & u_{60} &= u_{00}, & u_{62} &= u_{04}, \\ u_{63} &= -u_{05}, & u_{67} &= -u_{01}, & u_{72} &= -u_{14}, & u_{73} &= u_{15}, & u_{76} &= -u_{10}, & u_{77} &= u_{11}. \end{aligned} \tag{8}$$

Now, we have all the details to quantify the amount of the quantum correlations QCs , that may be generated between the qubits A, C and between B, C via Rashba interaction, as well as, the amount of the quantum correlation that may be gained or lost from the initial system ρ_{AB} .

3. Quantum Correlation (QCs)

In this section, we investigate the quantum correlations behavior by means of the negativity, \mathcal{N} [23]. It is well known that, the negativity is an accepted measure of entanglement between two-qubit system. However, for any two-qubit system ρ_{12} , the negativity, \mathcal{N}_{eg} is defined as,

$$\mathcal{N}_{eg} = 2 \sum_{i=1}^4 \max(0, -\mu_i), \quad (9)$$

where μ_i are the negative eigenvalue of the partial transpose of the state ρ_{12} [23] [24] [25]. For the maximal entangled state (MES), the negativity $\mathcal{N}_{eg} = 1$, while it is zero for the separable states and $0 < \mathcal{N}_{eg} \leq 1$ for partial entangled states (PES).

3.1. Quantum Correlation of $\rho_{AB}(t)$

The behavior of the QCs , between the qubits A and B is described in **Figure 1(a)**, where it is assumed that, the two-qubit system $\rho_{AB}(0)$ is initially prepared in a maximum entangled state (MES), while the qubit C , is prepared in a product state such that $\rho_c = |0\rangle\langle 0|$ and different values of the coherence parameter κ are considered. It is clear that, at $t=0$, the negativity \mathcal{N} oscillates between its upper and lower bounds, where the upper bounds are displayed at large κ , namely at large degree of coherence. Moreover, the phenomenon of the entanglement death/birth are displayed periodically, where the predicted time interval of its disappearance at small κ is large, while it disappears temporary as one increases the coherence of the initial state. **Figure 1(b)** describes the behavior of the negativity at different initial state settings, where it is assumed that, the two-qubit system ρ_{AB} is prepared in a maximum entangled state (MES), while the qubit C is prepared in a superposition pure state. The negativity behavior is similar to that displayed in **Figure 1(a)**, but the possibility of vanishing the QCs decreases at small values of the coherence parameter κ , while at large κ it doesn't vanish. Moreover, the number of oscillations decreases and the minimum values of the non-vanishing entanglement are better than those displayed in **Figure 1(a)**.

To investigate the effect of Rashba interaction strength, **Figure 2** is plotted at small value of this strength, where we set $\zeta = 0.2$. It is shown that, the amount of QCs are more robust than those displayed in **Figure 1(a)**, where the number of oscillations is small. However, at small values of κ , namely the state ρ_{AB} has a small degree of coherence, the possibility that the state turns into a product state increases, where as it is observed from **Figure 2**, the vanishing interval time of the QCs increases as one increases κ .

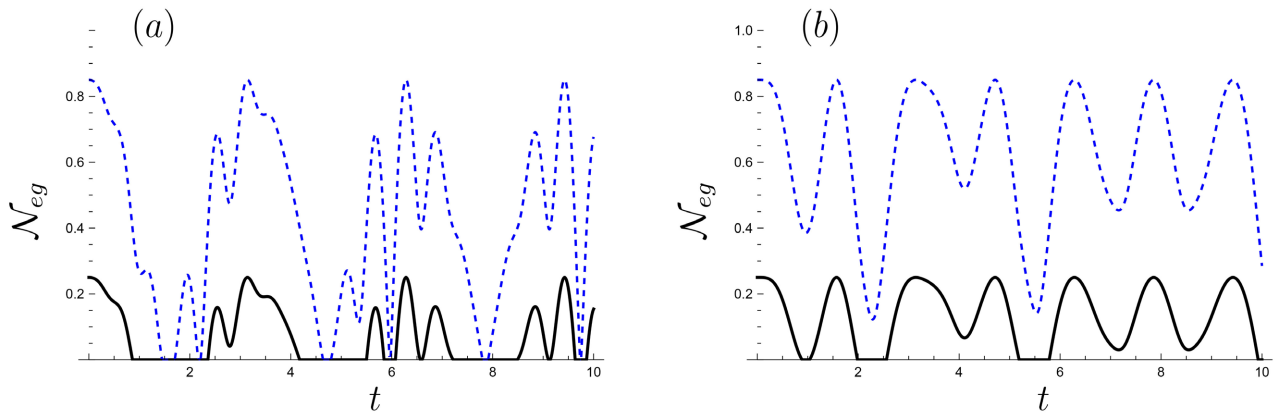


Figure 1. The amount of quantum correlation of the state $\rho_{ab}(t)$ that is quantified by using the negativity. The sold (black), and the dash (blue) curves are evaluated at $\kappa=0.5, 0.9$, respectively, where we set $\omega=2$, $\zeta=0.5$, $\varepsilon=0.2$, $\beta=0.4$, and (a) $\alpha=\frac{\pi}{4}$, $\gamma=0$, and (b) $\alpha=\frac{\pi}{4}$, $\gamma=\frac{\pi}{4}$.

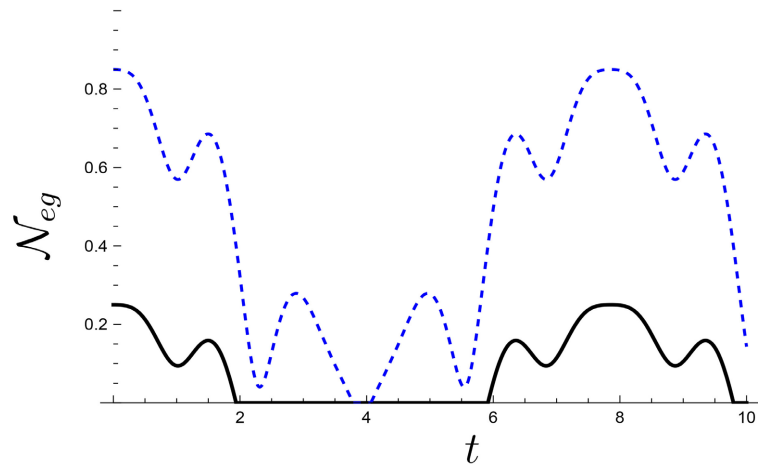


Figure 2. The same as **Figure 1(a)** but we set $\zeta=0.2$.

In **Figure 3**, the impact of the Rashba interaction’s strength on the generated entanglement between the two qubits A and B is discussed. Different values of ζ are considered, where it is assumed that the two-qubit systems are initially prepared in a product state. Due to the spin interaction between the two-qubit system, there will be an entangled state will be generated. Moreover, at the same time Rashba interaction is switched on between the qubits A and C . The amount of QCs that may be contained in the state ρ_{AB} depends on strength ζ , where at small values of ζ , the possibility of generating an entangled state ρ_{AC} with large degree of QCs , decreases, and accordingly the possibility that ρ_{AB} has a large QCs increases. This phenomenon has displayed clearly by comparing **Figure 3(a)**, and **Figure 3(b)**, where we set $\zeta=0.2, 0.5$, respectively. Moreover, the degree of coherence that is characterized by the parameter κ , plays an essential role on the behavior of the QCs , where the long-lived quantum correlations are displayed at large values of κ .

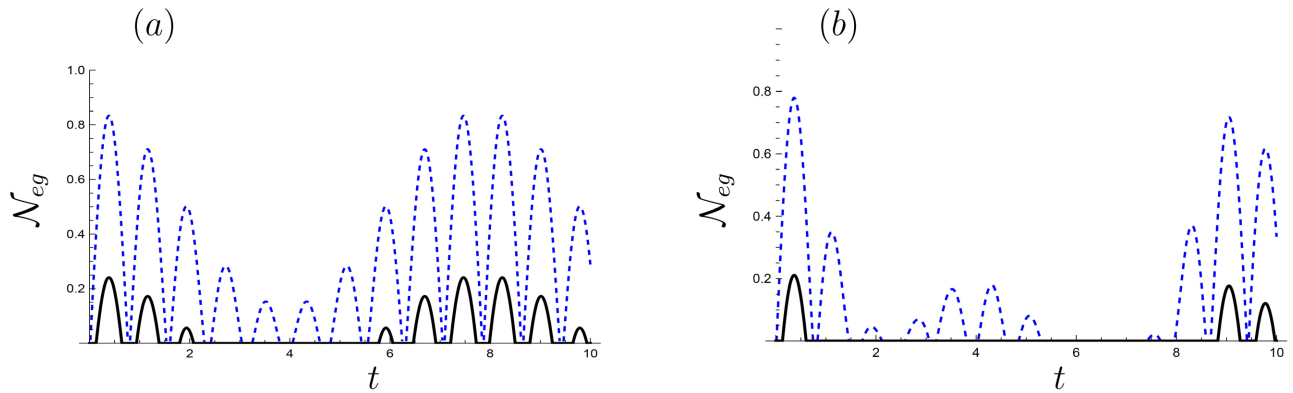


Figure 3. The amount of quantum correlation of the state $\rho_{ab}(t)$ that is quantified by using the negativity. The solid (black), and the dash (blue) curves are evaluated at $\kappa=0.5, 0.9$, respectively, where we set $\omega=2$, $\varepsilon=0.2$, $\beta=0.2$, $\alpha=0$, $\gamma=0$ (a) $\zeta=0.2$ (b) $\zeta=0.5$.

In **Figure 4**, we investigate the impact of the spin interaction parameter between the two qubits A and B in the presence of Rashba interaction. It is clear that, at small values of the Rashba interaction ζ , the entanglement between the two qubits are generated as soon as the interaction is switched on. However, at large values of ζ , the QCs between the two qubits will be generated at large interaction time. These results can be observed by comparing **Figure 4(a)** and **Figure 4(b)**. Moreover, the disappearance interval of the QCs that depicted at large value of Rashba strength are larger than those displayed at small values of this strength. Furthermore, the maximum bounds of the QCs that displayed in **Figure 4(b)** are smaller than those shown in **Figure 4(a)**.

From **Figure 4**, one may conclude that, due to the interaction between the two qubits A and C via Rashba interaction, the entanglement that it has generated between the qubits A and B not only depends on the spin interaction, but also on Rashba strength. However, it has an essential role as a control parameter to increase/decrease the entanglement between the two qubits A and B . Moreover, from **Figure 3** and **Figure 4**, it is clear that, the possibility of generating quantum correlations between the two qubits A and B increases as one increases the spin interaction strength ω .

3.2. Quantum Correlation of $\rho_{AC}(t)$

In this subsection, we investigate the impact of the Rashba strength on the generated quantum correlations between the qubits A and C via direct interaction. **Figure 5**, displays the behavior of the negativity as a quantifier of the QCs , at different values of ζ , where it is assumed that, the three qubits are separable. There is an entangled state is generated between the two qubits A and C , as the interaction is switched on. Similarly, the upper bounds depend on the values of the coherence parameter κ , where the largest values of the QCs are displayed at large κ . Moreover, the periodic behavior, sudden birth/death are displayed regularly.

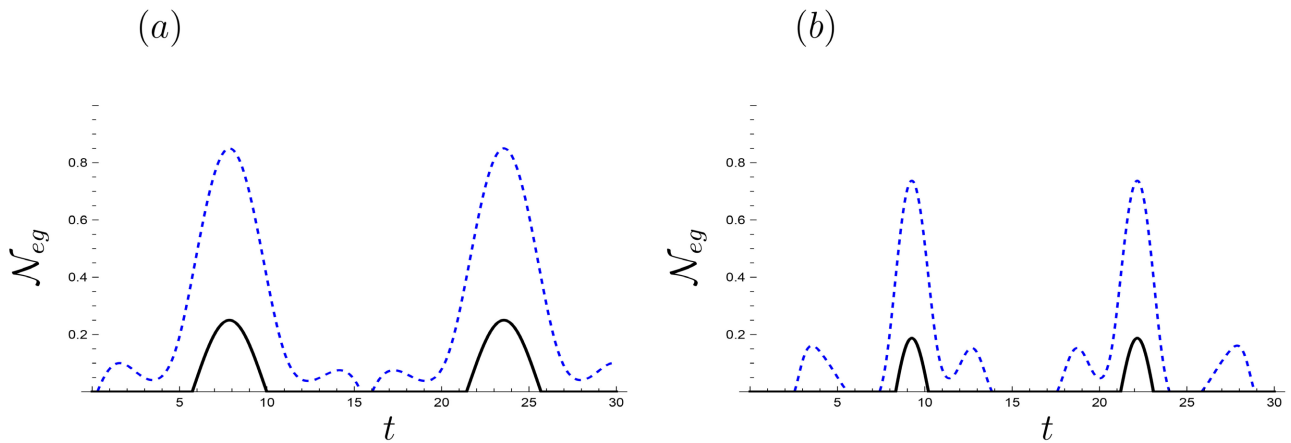


Figure 4. The same as **Figure 3**, but we set $\omega = 0.1$.

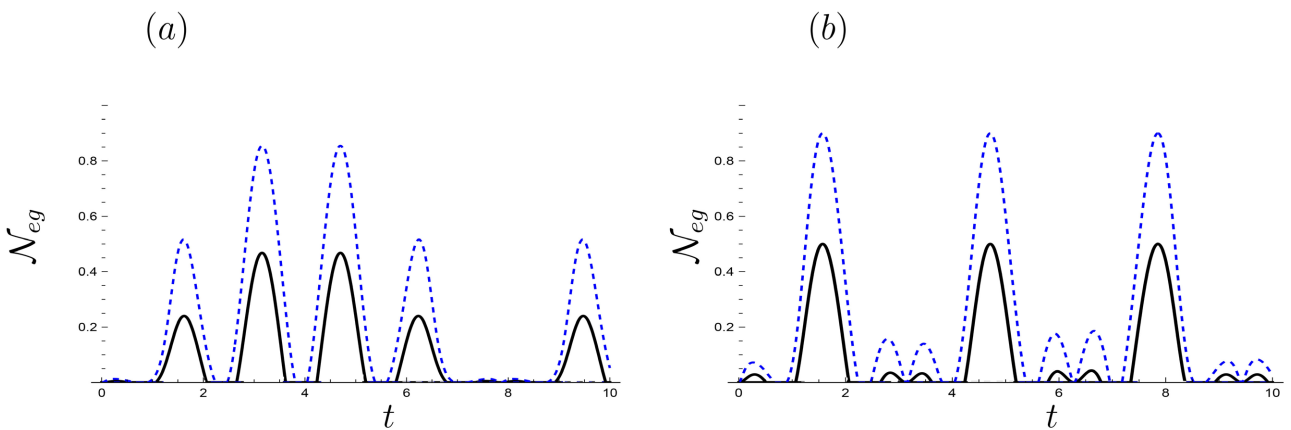


Figure 5. The negativity of the state ρ_{AC} , black line $\kappa = 0.5$, blue line $\kappa = 0.9$. $w = 2$, $\varepsilon = 0.2$, $\beta = 0.2$, $\alpha = 0$, $\gamma = 0$ (a) $\zeta = 0.2$, and (b) $\zeta = 0.5$.

The impact of the strength ζ on the amount of the quantum correlations that is contained in the state ρ_{AC} can be seen by comparing **Figure 5(a)** and **Figure 5(b)**, where we set $\zeta = 0.2, 0.5$, respectively. It is shown that, at large value of ζ , an entangled state between the qubits A and C is generated in a short interaction time compared with that displayed at small values of ζ . Also, at small values of ζ , the predicted quantum correlation oscillates faster than those displayed at large ζ . This means that, the predicted exchanged correlations increase at small value of the Rashba strength.

From **Figure 3** and **Figure 5**, one may deduced that, due to the phenomena of exchanging the quantum correlation between the three qubits, if the predict QCs are large for ρ_{AB} , it will be small for ρ_{AC} . Moreover, if it vanishes completely in one state, it appears for the other state. The exchanging rate depends on the spin strength ω and Rashba strength ζ .

The entangling power of Rashba interaction in the presences of the spin interaction at a small strength is displayed in **Figure 6**, where we set $\omega = 0.1$. **Figure 6(a)**, shows that, due to the small strength values of the spin interaction, the quantum correlations between A and C are generated suddenly as soon as the

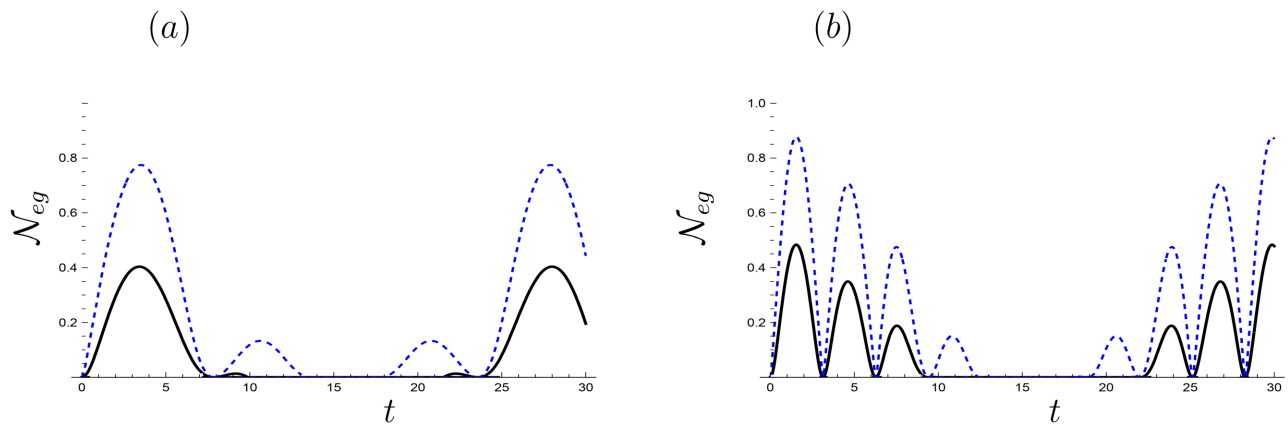


Figure 6. The same as **Figure 5**, but we set $\omega = 0.1$.

interaction is switched on, while as it is displayed from **Figure 5(a)**, the *QCs* are generated at longer interaction time, where we set $\omega = 0.2$. The numbers of oscillations are very small, namely a long-lived entanglement is generated between the two qubits *A* and *C*. **Figure 6(b)**, depicts the amount of quantum correlations that has contained in the state ρ_{AC} at large value of Rashba strength, where we set $\zeta = 0.5$. The displayed behavior shows that, the upper bounds are larger than those displayed in **Figure 6(a)**. Moreover, the oscillations' numbers are larger, namely the quantum correlations are exchanged faster.

3.3. Quantum Correlation of $\rho_{BC}(t)$

Similarly, in this subsection the behavior of the *QCs*, that may be generated between the qubits *B* and *C* indirectly via Rashba interaction is discussed, where we consider the same initial state settings and the same values of the interaction parameters.

In **Figure 7**, the *QCs* that are contained in the state ρ_{BC} are investigated at different values of Rashba interaction's strength. The behavior is similar to that displayed for ρ_{AB} and ρ_{AC} , where the phenomena of the sudden changes (death/birth) are displayed. The maximum bounds of the *QCs* that shown in **Figure 7(a)** are larger than those displayed in **Figure 7(b)**. This means that, large values of Rashba force reduce the amount of entanglement present in the case ρ_{BC} .

The effect of the Rashba interaction in the presences of smaller values of the spin interaction on the amount of *QCs* of the state ρ_{BC} is displayed in **Figure 8**, where we set $\omega = 0.1$. As it is observed from **Figure 7(b)** and **Figure 8(b)**, at the small values of ω and large values of ζ , the predict quantum correlations are much better than those shown at large values of ω .

4. The Non-Markovianity of the Three Partitions

In this section the effect of the Rashba and spin interactions strengths on the non-Markovianity of the three quantum states is investigated. It is well know

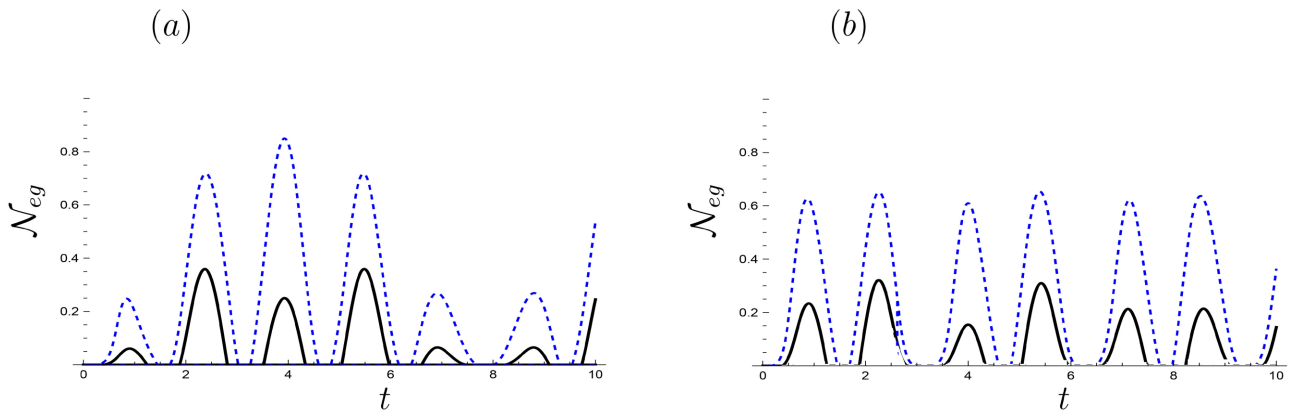


Figure 7. The negativity of ρ_{BC} , black line $\kappa=0.5$, blue line $\kappa=0.9$. $w=2$, $\varepsilon=0.2$, $\zeta=0.5$, $\beta=0.2$, $\alpha=0$, $\gamma=0$ (a) $\zeta=0.2$ and (b) $\zeta=0.5$.

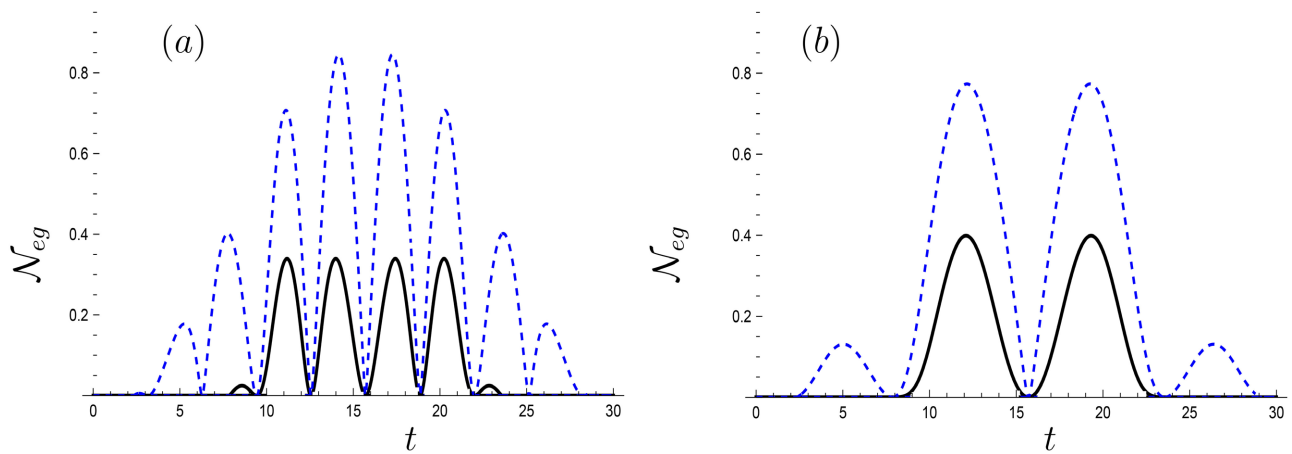


Figure 8. The same as **Figure 7**, but we set $\omega=0.1$.

that, it is difficult to isolate a quantum system from its environment, which leads to the non-Markovian behavior and eventually a back-flow of information from the environment into the system can be observed. The non-Markovianity of the system can be described by [26] [27] [28],

$$\mathcal{N}(\rho) = \max_{\rho_{i,j}(0)} \int_{\sigma>0} \frac{d}{dt} D(\rho_i(t), \rho_j(t)) dt, \tag{10}$$

where $D(\rho_i(t), \rho_j(t)) = \frac{1}{2} \text{tr} |\rho_i(t) - \rho_j(t)|$, $i, j = A, B$ and C .

Figure 9 displays the behavior of $\mathcal{N}_{\rho_i}, i = AB, AC$ and BC at small value of the spin interaction, where we set $\omega = 0.1$. The general behavior shows that, \mathcal{N}_{ρ_i} increases as soon as the interaction is switched on to reach its maximum value. The smallest maximum bound is depicted for ρ_{AB} , while the largest bound of the \mathcal{N}_{ρ_i} is observed for ρ_{AC} . Moreover the maximum peaks of the non-Markovianity of the state ρ_{AB} appear simultaneity as the minimum packs of $\mathcal{N}_{\rho_{AC}}$ and $\mathcal{N}_{\rho_{BC}}$ are displayed. The non-Markovianity vanishes for all the three partitions at the same interaction time, namely the exchanging process is frozen. There is no a remarkable fast oscillation behavior, namely the rate of changing

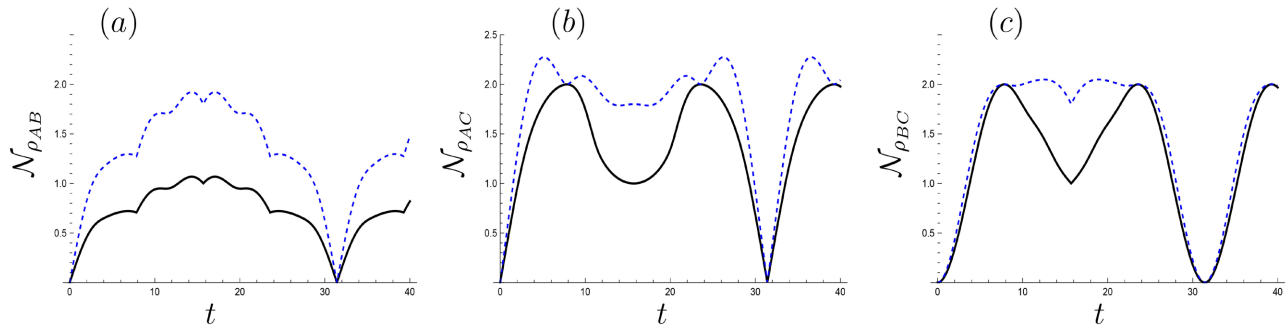


Figure 9. The non-Markovianity for the three states (a) ρ_{AB} , (b) ρ_{AC} , and (c) ρ_{BC} . The solid (black), and dot (blue) curves are evaluated at line $\kappa = 0.5, 0.9$, respectively, where we set $\omega = 0.1$, $\varepsilon = 0.2$, $\beta = 0.2$, $\zeta = 0.2$, $\alpha = 0$, $\gamma = 0$.

systems non-Markovianity is small. The increasing rate the non-Markovianity of state that generated by direct interaction with Rashba interaction is larger than that displayed by indirect interaction.

To investigate the impact of Rashba interaction on the Markovianity, we set a large value of the strength ζ as it is shown in **Figure 10**, where we set $\zeta = 0.5$. The displayed behavior of ρ is similar to that shown in **Figure 9**. However, the upper bounds that have been displayed in **Figure 10** are larger than those shown in **Figure 9**. Moreover, the number of oscillations and their amplitudes are large compared with their corresponding ones in **Figure 9**. As an observation, the vanishing interaction time of the non-Markovianity doesn't depend on the strength of Rashba interaction, where it vanishes at the same time.

From **Figure 9** and **Figure 10**, one may induced that, the large values of Rashba strength increase the number of oscillations and their amplitudes. This means that, the memories of all the three partitions are unstable, where there will be a fast exchange of the physical properties between the three systems. Moreover, the memory of two qubit system, ρ_{AB} is more robust than that shown for ρ_{AC} and ρ_{BC} , which has generated via direct and indirect interaction. Also, when the minimum peaks are displayed on the behavior of $\mathcal{N}_{\rho_{AB}}$, the maximum peaks are appeared in $\mathcal{N}_{\rho_{AC}}$, $\mathcal{N}_{\rho_{BC}}$.

To clarify the effect of the spin interaction parameter on the non-Markovianity of the three partition, we set $\omega = 2$ in **Figure 11**, namely we increase the strength of the spin interaction between the qubits A and B . In general, \mathcal{N}_{ρ_i} oscillates faster than that has shown at all values of ω , *i.e.*, the exchanging process of QCs and information are faster. However, as it is displayed from **Figure 11(a)** and **Figure 11(b)**, the non-Markovianity of ρ_{AC} and ρ_{BC} are more stable than that shown for ρ_{AB} , where the period of changing $\mathcal{N}_{\rho_{AB}}$ is smaller than that depicted for $\mathcal{N}_{\rho_{AC}}$ and $\mathcal{N}_{\rho_{BC}}$. The non-Markovianity of ρ_{AB} vanishes at a shorter interaction time compared with that displayed for the other partitions. The coherence parameter has a clear effect on $\mathcal{N}_{\rho_{AB}}$ and $\mathcal{N}_{\rho_{BC}}$, where it displays a faster oscillations than that depicted for $\mathcal{N}_{\rho_{AC}}$.

5. Information Dynamics

In this section, we investigate the behavior of the information that encoded on

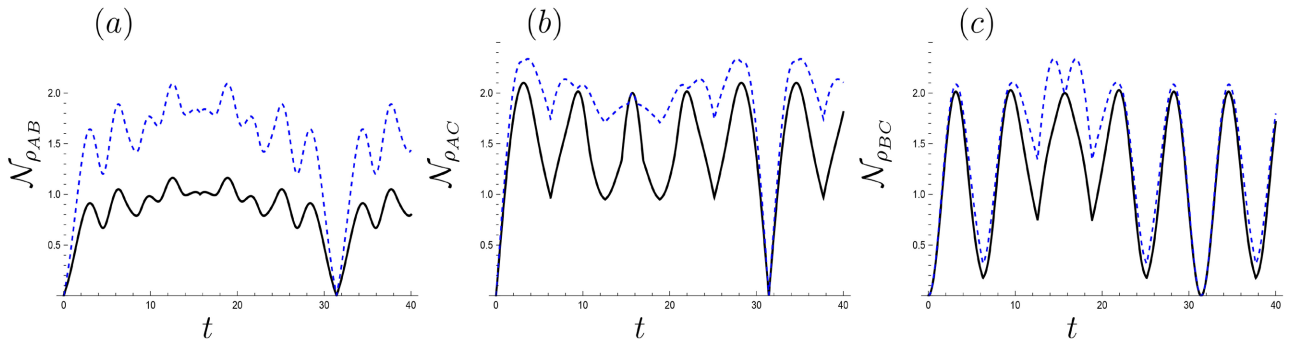


Figure 10. The same as Figure 9, but at $\zeta = 0.5$.

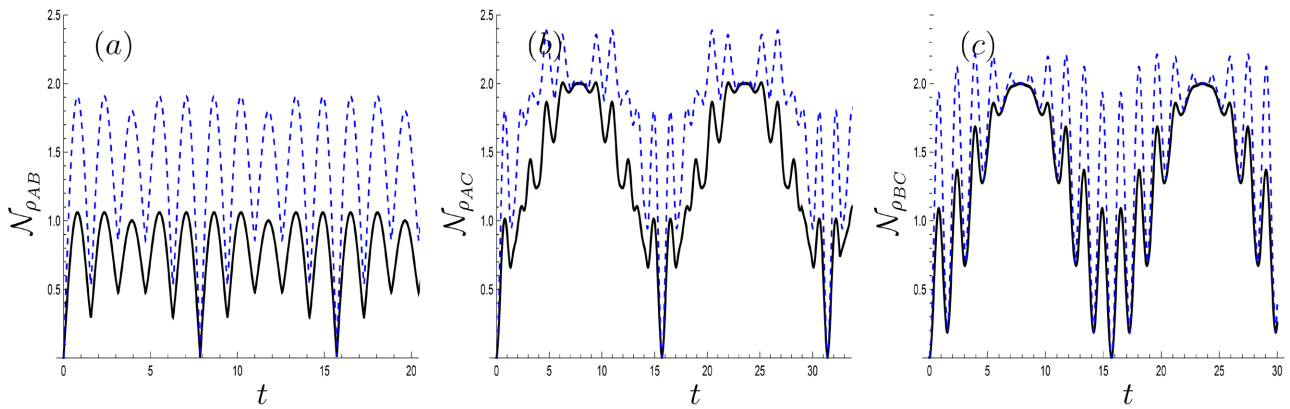


Figure 11. The same as Figure 9, but at $\omega = 2$.

each partition, where it is assumed that the two-qubit system, ρ_{AB} and the blank qubits are initially prepared in a product state. The amount of information is defined by [29] [30] [31],

$$\mathcal{I}_{\rho_i} = \log_2 D_i - \mathcal{S}(\rho_i), i = AB, AC, BC, \tag{11}$$

where $\mathcal{S}(\rho_i) = -\sum_j \lambda_j \log \lambda_j$ is the von-Neumann entropy, and λ_i are the eigenvalues of ρ_i . Figure 12 displays the effect of the spin and Rashba strengths on the behavior of \mathcal{I}_{ρ_i} . The general behavior shows that, the coherence parameter κ plays an essential role on increasing/decreasing the upper and lower bounds of \mathcal{I}_{ρ_i} , where the small values of κ decrease the oscillations amplitudes, while it increases as one increases κ . This coherence parameter has a different effect on the three partitions.

The effect of the Rashba interaction in the presence of different values of the spin strength can be deduced from Figure 13. The dynamics of the information that encoded in the three partitions at $\omega = 0.1$ and $\zeta = 0.2$ are displayed in Figure 13(a). It is shown that, for all the three states, \mathcal{I}_{ρ_i} decreases as soon as the interaction is switched on. At further interaction time, \mathcal{I}_{ρ_i} increases and decreases simultaneously. As the minimum bounds of $\mathcal{I}_{\rho_{AB}}$ and $\mathcal{I}_{\rho_{AC}}$ are depicted, the encoded information in $\mathcal{I}_{\rho_{BC}}$ reaches its maximum bound. Similarly, the maximum bounds are displayed for $\mathcal{I}_{\rho_{AC}}$, when the $\mathcal{I}_{\rho_{AB}}$ and $\mathcal{I}_{\rho_{BC}}$ are minimum. The regular oscillations are predicted on the behavior of the information the encoded in ρ_{AB} .

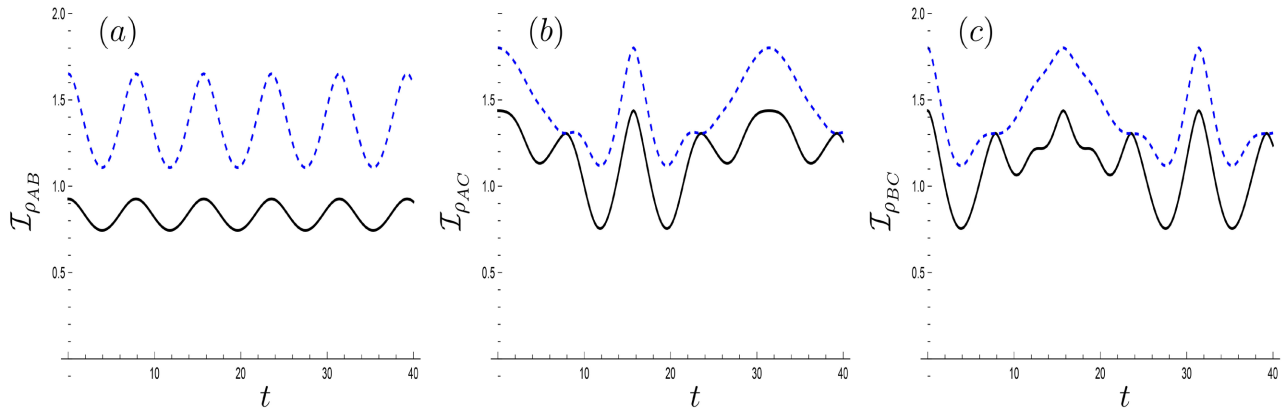


Figure 12. The behavior of the non-local information (a) $\mathcal{I}_{\rho_{AB}}$, (b) $\mathcal{I}_{\rho_{AC}}$, and (c) $\mathcal{I}_{\rho_{BC}}$, ρ_{AB} , black line $\kappa = 0.5$ and blue line $\kappa = 0.9$, $\omega = 0.1$, $\varepsilon = 0.2$, $\beta = 0.2$, $\zeta = 0.2$, $\alpha = 0$, $\gamma = 0$.

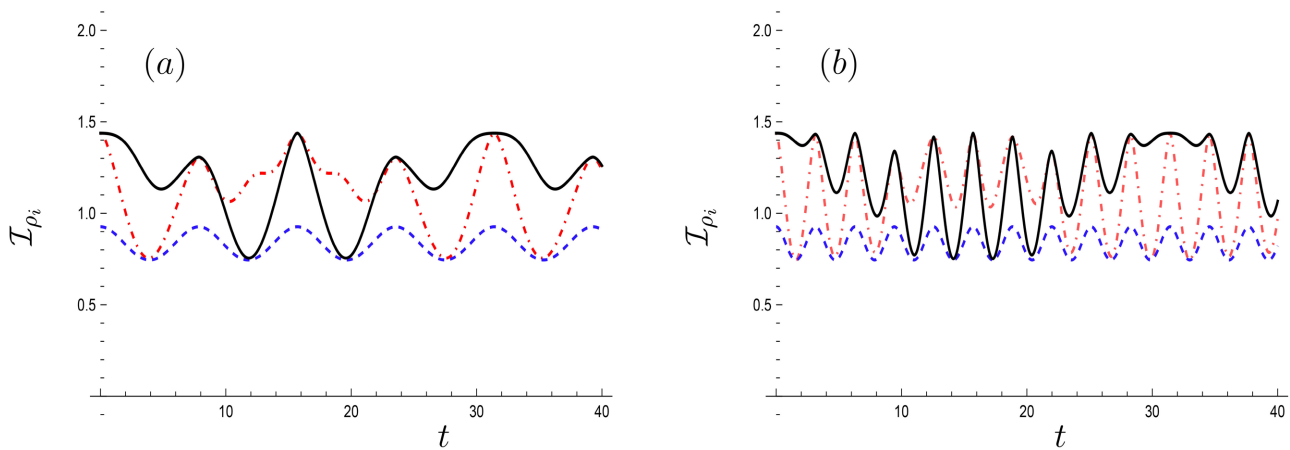


Figure 13. The behavior of \mathcal{I}_{ρ_i} , where we set $\kappa = 0.5$, $\varepsilon = 0.2$, $\beta = 0.2$, $\alpha = 0$, $\gamma = 0$. The dot, dash dot, and solid for ρ_{AB} , ρ_{BC} and ρ_{AC} , respectively where (a) $\omega = 0.1$, $\zeta = 0.2$, (b) $\omega = 0.1$, $\zeta = 0.5$.

Figure 13(b) displays the behavior of \mathcal{I}_{ρ_i} at large value of Rashba strength, where we set $\zeta = 0.5$. It is clear that, the fluctuations of the information between its lower and upper bounds increase, without any changes on the values of these bounds. It only increases the exchanging rate of information of the three qubits system.

6. Conclusions

The power of the Rashba interaction to generate entangled state between a three qubits system in the presence of the spin interaction is investigated. This idea is clarified by considering a two-qubit system ρ_{AB} which is initially prepared in a product, partially entangled, or maximum entangled states. Additionally, the qubit A interacts locally with another qubit C by using Rashba interaction. Due to these interactions, there are three quantum states have been created. Therefore, we investigate the behavior of the exchanged quantum correlations between the three states, their degree of non-Markovianity, and the amount of the scrambled information from/into these states.

The obtained results show that, the predicted quantum correlations for all the three states oscillate between their upper and lower bounds. The maximum bounds depend on the initial degree of coherence, where at small value of the coherence parameter, the upper bounds are smaller than those displayed at large values of this coherence parameter. Moreover, the interval time of vanishing these correlations for all the three states, increases at small coherence parameter. The phenomena of the sudden changes (death/birth) have been displayed periodically during the interaction time.

The effect of the Rashba strength on the behavior of the quantum correlations that may be generated between the three partitions is investigated. It is shown that, as one increases Rashba strength, the quantum correlations that have been generated directly between the qubits A and C increase on the expense of the amount of quantum correlations between the other partitions. However, this behavior will be changed if one increases the spin interaction's strength. Moreover, the robustness of these quantum correlations increases as one increases the strength of Rashba interaction, where the oscillations decrease, and consequently the long-lived quantum correlations are observed.

It is shown that, the non-Markovianity of the three partitions increases as soon as the interaction is switched on. The results show that, the memory of the initial entangled two qubit system is more robust than the others, where the predicted oscillations are very small, while for the other two partitions the non-Markovianity exchanges fast with a large rate, due to the large amplitudes of these oscillations. The non-Markovianity of the three partitions vanishes at the same interaction time, namely at this time, there is no exchanging process depicted. It is worth to mention that, the large values of the Rashba strength increase the oscillations and their amplitudes, and consequently the exchanging rate of the quantum information between the three qubits increases.

The coherence parameter plays an essential role on minimizing or maximizing the non-Markovianity properties of the evolved three partitions. The maximum bounds of the non-Markovianity that depicted at large coherence parameter are larger than those displayed at small values of this coherence parameter. At small values of the coherence parameter, the non-Markovianity of the entangled state that generated via direct or indirect interaction oscillates fast. This means that, the memories of these states are unstable, and consequently the possibility of exchanging the quantum correlations and information increases.

It is worth to shed the light on the effect of the spin interaction strength on the behavior of the non-Markovianity of the three partitions. The results show that, at large values of this strength, the non-Markovianity of the three partitions oscillates fast. Moreover, the predicted periodic time of these oscillations depends on whether these partitions are generated by direct or indirect interaction, and consequently the possibility of exchanging the physical properties between the three partitions will be different.

The information scrambling between the three qubit systems is discussed by

investigating the effect of Rashba interaction on the rate of exchanging process of information. It is shown that, the Rashba strength increases the oscillations of evolved information during the interaction time, and consequently the rate of exchanging the information between the three qubit increases. However, there is no noticeable effect on the upper and lower bounds of the amount of encoded information in the three partitions.

Conflicts of Interest

The authors declare no conflicts of interest regarding the publication of this paper.

References

- [1] Nielsen, M.A. and Chuang, I.L. (2019) Quantum Computation and Quantum Information. Cambridge University Press, Cambridge.
- [2] Cariolaro, G. (2015) Quantum Communications. Springer, Cham.
<https://doi.org/10.1007/978-3-319-15600-2>
- [3] Dotsenko, I.S. and Korobka, R. (2018) Entanglement Swapping in the Presence of White and Color Noise. *Communications in Theoretical Physics*, **69**, 143-153.
<https://doi.org/10.1088/0253-6102/69/2/143>
- [4] Eid, A. and Metwally, N. (2023) Entangled Kernel of Coded Information Using Quantum String. *International Journal of Quantum Information*, **21**, Article ID: 2350034.
<https://doi.org/10.1142/S021974992350034X>
- [5] Yu, T. and Eberly, J.H. (2009) Sudden Death of Entanglement. *Science*, **323**, 598-601.
<https://doi.org/10.1126/science.1167343>
- [6] Radwan, A., El-Shahat, T. and Metwally, N. (2020) Restrain the Losses of the Entanglement and the Non-Local Coherent Quantum Advantage of Accelerated Quantum Systems. *Optik*, **220**, Article ID: 165190.
<https://doi.org/10.1016/j.ijleo.2020.165190>
- [7] Ferreira, M., Rojas, O. and Rojas, M. (2023) Thermal Entanglement and Quantum Coherence of a Single Electron in a Double Quantum Dot with Rashba Interaction. *Physical Review A*, **107**, Article ID: 052408.
<https://doi.org/10.1103/PhysRevA.107.052408>
- [8] Yu, T. and Eberly, J.H. (2002) Phonon Decoherence of Quantum Entanglement, Robust and Fragile States. *Physical Review B*, **66**, Article ID: 193306.
<https://doi.org/10.1103/PhysRevB.66.193306>
- [9] Yu, T. and Eberly, J.H. (2004) Finite-Time Disentanglement via Spontaneous Emission. *Physical Review Letters*, **93**, Article ID: 140404.
<https://doi.org/10.1103/PhysRevLett.93.140404>
- [10] Metwally, N. (2014) Single and Double Changes of Entanglement. *Journal of the Optical Society of America B-Optical Physics*, **31**, 691-696.
<https://doi.org/10.1364/JOSAB.31.000691>
- [11] Dür, W. and Briegel, H.J. (2004) Stability of Macroscopic Entanglement under Decoherence. *Physical Review Letters*, **92**, Article ID: 180403.
<https://doi.org/10.1103/PhysRevLett.92.180403>
- [12] Ding, Y., Xie, S. and Eberly, J.H. (2021) Sudden Freezing and Thawing of Entanglement Sharing in a Shrunk Volume. *Physical Review A*, **103**, Article ID: 032418.
<https://doi.org/10.1103/PhysRevA.103.032418>

- [13] Metwally, N. and Ebrahim, F. (2020) Fisher Information of Accelerated Two-Qubit System in the Presence of the Color and White Noisy Channels. *International Journal of Modern Physics B*, **34**, Article ID: 2050027. <https://doi.org/10.1142/S0217979220500277>
- [14] Chiang, K.T. and Zhang, W.M. (2021) Non-Markovian Decoherence Dynamics of Strong-Coupling Hybrid Quantum Systems: A Master Equation Approach. *Physical Review A*, **103**, Article ID: 013714. <https://doi.org/10.1103/PhysRevA.103.013714>
- [15] He, Z., Zou, J., Li, L. and Shao, B. (2011) Effective Method of Calculating the Non-Markovianity N for Single-Channel Open Systems. *Physical Review A*, **83**, Article ID: 012108. <https://doi.org/10.1103/PhysRevA.83.012108>
- [16] Wang, Y., Hao, Z.Y., Li, J.K., Liu, Z.H., Sun, K., Xu, J.S., Li, C.F. and Guo, G.C. (2023) Observation of Non-Markovian Evolution of Einstein-Podolsky-Rosen Steering. *Physical Review Letters*, **130**, Article ID: 200202. <https://doi.org/10.1103/PhysRevLett.130.200202>
- [17] Heide, M., Bihlmayer, G. and Blügel, S. (2008) Dzyaloshinskii-Moriya Interaction Accounting for the Orientation of Magnetic Domains in Ultrathin Films: Fe/W(110). *Physical Review B*, **78**, Article ID: 140403. <https://doi.org/10.1103/PhysRevB.78.140403>
- [18] Qiang, Z., Zhang, X.P., Zhi, Q.J. and Ren, Z.Z. (2009) Entanglement Dynamics of a Heisenberg Chain with Dzyaloshinskii-Moriya Interaction. *Chinese Physics B*, **18**, 3210-3214. <https://doi.org/10.1088/1674-1056/18/8/019>
- [19] Hayakawa, Y., Imai, Y. and Kohno, H. (2023) Dzyaloshinskii-Moriya Interaction in Strongly Spin-Orbit Coupled Systems: General Formula and Application to Topological and Rashba Materials. *Physical Review B*, **108**, Article ID: 064409. <https://doi.org/10.1103/PhysRevB.108.064409>
- [20] Oliveira, I.S., Bonagamba, T.J., Sarthour, R.S., Freitas, J.C.C. and deAzevedo, E.R. (2007) NMR Quantum Information Processing. Elsevier, Oxford.
- [21] Mohammed, A.R., Ahmed, A.H., El-Shahat, T.M. and Metwally, N. (2021) Quantum Steering over an Entangled Network That Is Generated *via* Dipolar Interaction. *Physica A: Statistical Mechanics and Its Applications*, **584**, Article ID: 126380. <https://doi.org/10.1016/j.physa.2021.126380>
- [22] Molenkamp, L.W., Schmidt, G. and Bauer, W. (2001) Rashba Hamiltonian and Electron Transport. *Physical Review B*, **64**, Article ID: 121202. <https://doi.org/10.1103/PhysRevB.64.121202>
- [23] Horodecki, P. (1997) Separability Criterion and Inseparable Mixed States with Positive Partial Transposition. *Physics Letters A*, **232**, 333-339. [https://doi.org/10.1016/S0375-9601\(97\)00416-7](https://doi.org/10.1016/S0375-9601(97)00416-7)
- [24] Berrada, K., El Baz, M., Eleuch, H. and Hassouni, Y. (2010) A Comparative Study of Negativity and Concurrence Based on Spin Coherent States. *International Journal of Modern Physics C*, **21**, 291-305. <https://doi.org/10.1142/S0129183110015129>
- [25] Metwally, N. (2021) Steering Information in Quantum Network. *3rd Smart Cities Symposium (SCS 2020)*. <https://doi.org/10.1049/icp.2021.1341>
- [26] Khan, N.A., Jan, M., Shah, M., Sajid, M., Zaman, Q., Ali, M. and Khan, D. (2022) Entanglement-Based Measure of Non-Markovianity in Relativistic Frame. *Optik*, **260**, Article ID: 169016. <https://doi.org/10.1016/j.jileo.2022.169016>
- [27] Hesabi, S., Afshar, D. and Paris, M.G.A. (2019) Non-Markovian Evolution of a Two-Level System Interacting with a Fluctuating Classical Field *via* Dipole Interaction. *Optics Communications*, **437**, 377-381. <https://doi.org/10.1016/j.optcom.2019.01.018>

- [28] Jan, M., Xu, X.Y., Wang, Q.Q., Chen, Z., Han, Y.J., Li, C.F. and Guo, G.C. (2019) Dipole-Dipole Interactions Enhance Non-Markovianity and Protect Information against Dissipation. *Chinese Physics B*, **28**, Article ID: 090303. <https://doi.org/10.1088/1674-1056/ab37f2>
- [29] Horodecki, M., Horodecki, P., Horodecki, R., Oppenheim, J., Sen(De), A., Sen, U. and Synak-Radtke, B. (2005) Local versus Nonlocal Information in Quantum-Information Theory: Formalism and Phenomena. *Physical Review A*, **71**, Article ID: 062307. <https://doi.org/10.1103/PhysRevA.71.062307>
- [30] Witten, E. (2020) A Mini-Introduction to Information Theory. *La Rivista Del Nuovo Cimento*, **43**, 187-227. <https://doi.org/10.1007/s40766-020-00004-5>
- [31] Abd-Rabbou, M.Y., Metwally, N., Ahmed, M.M.A. and Obada, A.S.F. (2019) Suppressing the Information Losses of Accelerated Qubit-Qutrit System. *International Journal of Quantum Information*, **17**, Article ID: 1950032. <https://doi.org/10.1142/S0219749919500321>